

available at www.sciencedirect.comjournal homepage: www.elsevier.com/locate/biochempharm

Regression of prostate cancer xenografts by RLIP76 depletion

Sharad S. Singhal^{*}, Cherice Roth, Kathryn Leake, Jyotsana Singhal,
Sushma Yadav, Sanjay Awasthi

Department of Molecular Biology and Immunology, University of North Texas Health Science Center, Fort Worth, TX 76107, United States

ARTICLE INFO

Article history:

Received 5 October 2008

Accepted 18 November 2008

Keywords:

RLIP76

Cancer

Drug-resistance

Xenografts

Glutathione-conjugate transport

ABSTRACT

RLIP76 plays a central role in radiation and chemotherapy resistance through its activity as a multi-specific ATP-dependent transporter which is over-expressed in a number of types of cancers. RLIP76 appears to be necessary for cancer cell survival because both *in vitro* cell culture and *in vivo* animal tumor studies show that depletion or inhibition of RLIP76 causes selective toxicity in malignant cells. RLIP76 induces apoptosis in cancer cells through the accumulation of endogenously formed GS-E. The results of our *in vivo* studies demonstrate that administration of RLIP76 antibodies, siRNA or anti-sense to mice bearing xenografts of PC-3 prostate cancer cells leads to near complete regression of established subcutaneous xenografts with no apparent toxic effects. Since anti-RLIP76 IgG (which inhibit RLIP76-mediated transport), siRNA and antisense (which deplete RLIP76) showed similar tumor regressing activities, our results indicate that the inhibition of RLIP76 transport activity at the cell surface is sufficient for observed anti-tumor activity. These studies indicate that RLIP76 serves a key effector function for the survival of prostate cancer cells and that it is a valid target for cancer therapy.

© 2008 Elsevier Inc. All rights reserved.

1. Introduction

Prostate cancer is the most frequently diagnosed malignancy and the second leading cause of cancer-related deaths in men in the U.S. In the early stage of the disease, the treatments of choice are extensive surgery and/or radiation therapy. Although both treatment modalities are effective, they are associated with significant morbidity and mortality. Despite striking improvements in drug therapy targeting kinase signaling pathways, prostate cancer remains a deadly malignancy if not found and removed in early stages. It is characteristically so highly drug-resistant, that no effective

and life-prolonging regimen of cytotoxic chemotherapy has been demonstrated for prostate cancer despite several decades of effort. Although prostate cells characteristically express high levels of transporter proteins in their membranes that can contribute to drug-resistance, and may also play some role in radiation resistance, targeting the ATP Binding Cassette (ABC)-transporter family protein has not been effective reversing drug-resistance in prostate cancer [1,2]. Prostate cancer is being detected with increasing frequency, and many patients are receiving such treatments as radical prostatectomy and radiation therapy. The highly drug and radiation-resistant nature of prostate cancer, as compared

^{*} Corresponding author at: Department of Molecular Biology and Immunology, 3500 Camp Bowie Boulevard, 416 S RES Building, University of North Texas Health Science Center, Fort Worth, TX 76107-2699, United States. Tel.: +1 817 735 0459; fax: +1 817 735 2118.

E-mail address: ssinghal@hsc.unt.edu (S.S. Singhal).

Abbreviations: RLIP76 (RalBP1), Ral-interacting protein; GSH, glutathione; GS-E, glutathione-electrophile-conjugates; DNP-SG, dinitrophenyl S-glutathione; DOX, doxorubicin; 4HNE, 4-hydroxy-t-nonenal; IOVs, in-side out vesicles; MDR, multi-drug-resistance; Pgp, P-glycoprotein; MRP1, multi-drug-resistance associated protein; SCLC, small cell lung cancer; NSCLC, non-small cell lung cancer; POB1, partner of RalBP1; TUNEL, TdT-mediated dUTP nick end labeling assay.

0006-2952/\$ – see front matter © 2008 Elsevier Inc. All rights reserved.

doi:10.1016/j.bcp.2008.11.013

with other neoplasm such as lung or breast cancer, is a major reason why there is still no effective and life-prolonging traditional cytotoxic chemotherapy for prostate cancer [3–5].

Clinically, however, inhibitors of ABC-transporters have not yet been successful in improving chemotherapeutic outcomes [6,7], though alternative targeting strategies may ultimately prove clinically efficacious [8]. Clearly, other transport and resistance mechanisms are involved [9]. In contrast, genetic deletion of the non-ABC transporter, RLIP76, causes loss of about 4/5 of total transport activity for glutathione-conjugates (GS-E), along with major phenotypic effects due to sensitivity to stress or toxin mediated apoptosis. The loss of this transport activity for GS-E resulted in demonstrated accumulation of GS-E and their electrophilic precursors (e.g., GS-HNE and 4HNE) in the tissues of these animals [10].

Cell-line, animal and human clinical data indicate that the ABC-transporters MRP, P-glycoprotein (Pgp) and related transporters are clearly able to mediate drug-accumulation defects in cultured malignant cells, but correlations with pathology, clinical resistance and outcomes in prostate cancer are poor, and attempts at improving therapeutic efficacy by targeting these have not been successful [1,3–5]. Our approach will supply a missing piece of the puzzle to the understanding of multi-specific transport mechanisms in prostate cancer, a stress-responsive non-ABC, high capacity transporter, which must have had significant confounding effect in studies of ABC-transporters. Cancer cells appear significantly more sensitive to apoptosis triggered by blocking RLIP76 than normal cells, suggesting the feasibility of targeting RLIP76 in prostate cancer therapy.

RLIP76 was characterized as a human GTPase-activating protein, Ral-interacting protein. It was cloned as a Ral-binding GAP through a yeast two-hybrid screen [11]. It is a 76 kDa protein, but it appears as a 95 kDa band in SDS-PAGE [12]. Complete and sustained regression of human lung and colon cancer xenografts by systemic depletion clearly demonstrates the effectiveness of targeting the mercapturic acid pathway through RLIP76 [13]. Present studies were therefore designed to examine the effect of inhibiting transport activity of RLIP76 on PC-3 cells in culture and on tumor xenografts in nude mice. The focus of our present studies is to develop a novel therapeutic strategy for the treatment of prostate cancer by using RLIP76 antibody, siRNA or antisense.

2. Materials and methods

2.1. Materials

Bacterial strains DH5 α and BL21(DE3) were purchased from Invitrogen Life Tech. (Carlsbad, CA). pET30a(+), the T7 promoter based expression vector was purchased from Novagen, Inc. (Madison, WI). Restriction enzymes, thermostable DNA polymerase (Vent polymerase) and DNA ligase were from New England Biolabs (Beverly, MA). dNTPs were from Applied Biosystems (Foster city, CA). RPMI-1640 and DMEM medium, phosphate buffered saline (PBS), penicillin/streptomycin solution (P/S), fetal bovine serum (FBS), trypsin-EDTA, and trypan blue were purchased from GIBCO BRL Inc.,

Grand Island, NY. Dimethylsulfoxide (DMSO), G418 (geneticin) and 3-(4,5-dimethylthiazol-2-yl)-2,5-diphenyltetrazolium bromide (MTT) were obtained from sigma (St Louis, MO). Doxorubicin (DOX, adriamycin) was obtained from Adria Laboratories (Columbus, OH). ^3H -GSH (3000 Ci/mmol) was purchased from Pharmacia Biotech (Piscataway, NJ). ^{14}C -DOX (specific activity 44.8 Ci/mmol) was purchased from NEN Life Sciences (Boston, MA). Polyclonal rabbit-anti-human rec-RLIP76 IgG as well as pre-immune IgG were prepared and purified as described previously [12]. Secondary antibody for Western blots, goat anti-rabbit IgG horseradish peroxidase conjugate was purchased from Sigma (St. Louis, MO). TUNEL fluorescence detection kit was purchased from Promega (Madison, WI). DNP-SG was synthesized from CDNB and GSH according to the method described by us previously [14]. The sources of other chemicals used in this study were same as described previously [12].

2.2. Cell lines and cultures

Human SCLC H82, NSCLC H226 (squamous cell carcinoma), kidney Caki-2, prostate PC-3 and colon SW-480 from American Type Culture Collection (Manassas, VA), were used in these studies. Human aortic vascular smooth muscle cells (HAVSMC) and human umbilical vascular endothelial cells (HUVEC) were kindly provided by Dr. Paul Boor (UTMB, Galveston, TX) and Dr. Fiemu Nwariaku (UTSWMC, Dallas, TX), respectively. All cells were cultured at 37 °C in a humidified atmosphere of 5% CO $_2$ in the appropriate medium: RPMI 1640 (H82, H226, Caki-2, and SW-480), Ham's F12K (PC-3), DMEM (HAVSMC), and EGM-2 bullet kit (HUVEC) medium supplemented with 10% (v/v) heat-inactivated FBS and 1% (v/v) P/S solution.

2.3. Anti-RLIP76 antibodies

We have raised and purified polyclonal rabbit-anti-human RLIP76 IgG and aliquots were stored at –86 °C. All reagents for the preparation of antibodies and storage were filtered through 0.22 μm filters and handled under laminar flow hoods in a sterile manner. Aerobic, anaerobic and fungal cultures of random aliquots were performed at 2-month intervals. The integrity and purity of the antibodies were consistently checked by SDS-PAGE and Western-blot analysis against anti-IgG antibodies during these studies. Protein-A affinity purified immunoglobulin fraction obtained from the pre-immune serum was used as control. Anti-RLIP76 IgG used in these experiments was previously shown by Ouchterlony double immuno-diffusion assay to be non-cross-reactive with any other proteins including Pgp or MRP [15,16].

2.4. RLIP76 siRNA preparation

We chose aa 171–185 (nucleotide 510–555 starting from 1 AUG codon in the open reading frame) in the N-terminal region of RLIP76 as the target region to design for siRNA because of lack of homology with other proteins or nucleotide sequences. We searched for 23-nucleotide sequence motif, AA(N19)TT or NA(N21) (N, any nucleotide) and selected hits with approximately 50% GC contents. The sequence of sense siRNA

corresponds to N21. We converted 3' end of the sense siRNA to TT. The rationale for this sequence conversion was to generate a symmetric duplex with respect to the sequence composition of sense and antisense 3' overhangs. The antisense siRNA was synthesized as the complement to position 1–21 of the 23-nucleotide motif. The selected siRNA sequence was blast-search (NCBI database) against EST libraries, to ensure that only one gene is targeted. Chemically synthesized siRNA duplex in the 2' de-protected and desalted forms, was purchased from Dharmacon Research (Lafayette, CO). A 23 nucleotide long scrambled siRNA duplex was used as a control. The scrambled siRNA sequence was not homologous with RLIP76 mRNA in a blast-search against RLIP76. The siRNA duplex was re-suspended in 1X universal buffer, provided by Dharmacon Research Laboratory (Lafayette, CO). The targeted cDNA sequence (AAGAAAAAGCCAATTCAGGAGCC) corresponds to aa 170–176 (nt 508–528). The corresponding sense and antisense siRNA sequences are GAAAAAGCCAAUUCAGAGCCdTdT and GGCUCUGAAUUGGCUUUUCdTdT, respectively. The sequence of the scrambled siRNA in the sense and antisense directions are GUAACUGCAACGAUUUCGAUGdTdT and CAUCGAAAUCGUUGCAGUUACdTdT, respectively. Transfection of siRNA duplexes was performed using Transmessenger Transfection Reagent kit (Qiagen) and assay for silencing 24 h after transfection.

2.5. RLIP76 phosphorothioate anti-sense DNA preparation

The region spanning amino acid residues 171–185 (nucleotide 510–555 starting from 1 AUG codon in the open reading frame) in the N-terminal region of RLIP76 was chosen as the target region for synthesis of phosphorothioate DNA. The oxygen in the backbone of the DNA molecules was replaced by sulfur in each phosphate group, which makes the DNA backbone resistant to nucleases. However, the macromolecule remains electrically charged, impeding its passage across cell membrane. Selected DNA sequence was subjected to blast-search (NCBI database) against EST libraries, to ensure that only the selected gene was targeted. Chemically synthesized phosphorothioate DNA in desalted form was purchased from Biosynthesis Inc (Lewisville, TX). A 21 nucleotide long scrambled phosphorothioate DNA was used as a control. The scrambled DNA sequence was not homologous with RLIP76 cDNA in a blast-search against RLIP76. The targeted cDNA sequence (AAGAAAAAGCCAATTCAGGAGCC) corresponds to nt 508–528. The corresponding phosphorothioate DNA sequence was GGCTCCTGAATTGGCTTTTTC. The sequence of the scrambled DNA was CATCGAAATCGTTGCAGT-TAC. Transfection of phosphorothioate DNA was performed using Maxfect transfection reagent (Molecular) and assayed for silencing 24 h after transfection.

2.6. Drug sensitivity (MTT) assay

Cell number/ml in an aliquot of cells growing in log phase was determined by counting trypan blue excluding cells in a hemocytometer and 20,000 cells were plated into each well of 96-well flat-bottomed micro-titer plates. After 12 h incubation at 37 °C, medium containing either pre-immune IgG or anti-

RLIP76 IgG were added to cells. After 24–48 h incubation, 20 µl of 5 mg/ml MTT were introduced to each well and incubated for 2 h of exposure. The plates were centrifuged and medium was decanted. Cells were subsequently dissolved in 100 µl DMSO with gentle shaking for 2 h at room temperature, followed by measurement of optical density at 570 nm [17,18]. Eight replicate wells were used in each point in each of three separate measurements. Measured absorbance values were directly linked with a spreadsheet for calculation of IC₅₀, defined as the drug concentration that reduced formazan formation by 50%. Depletion of RLIP76 expression in cells by RLIP76 siRNA and RLIP76 antisense were measured as follows: cells were incubated for 3 h with 0–4 µg/well either RLIP76 siRNA or anti-sense in Transmessenger Transfection Reagent (Qiagen) and Maxfect transfection reagent (Molecular), respectively, according to the manufacturer provided protocol.

2.7. Cloning, prokaryotic expression, and purification of RLIP76

Purified RLIP76 protein (1965 bp; 655 aa) was obtained from *E. coli* BL21(DE3) expressing the pET30a(+) plasmid containing full-length cDNA corresponding to the sequence of RLIP76. The purification was carried out using DNPSG-affinity resin as described previously and purity was confirmed by SDS-PAGE and Western blot analyses [12].

2.8. Functional reconstitution of purified rec-RLIP76 into artificial liposomes and transport studies

Purified RLIP76 was dialyzed against reconstitution buffer (10 mM Tris-HCl, pH 7.4, 2 mM MgCl₂, 1 mM EGTA, 100 mM KCl, 40 mM sucrose, 2.8 mM BME, 0.05 mM BHT, and 0.025% polidocanol). An aqueous emulsion of soybean asolectin (40 mg/ml) and cholesterol (10 mg/ml) was prepared in the reconstitution buffer by sonication and 0.1 ml of this mixture was added to 0.9 ml aliquot of dialyzed purified rec-RLIP76 protein. The reaction mixture was sonicated at 50 W for 30 s. Vesiculation was initiated by addition of 200 mg SM-2 Bio-beads pre-equilibrated in the reconstitution buffer without polidocanol. Vesiculation was carried out for 4 h at 4 °C, followed by removal of SM-2 Bio-beads by centrifugation and the vesicles (RLIP76-liposomes) were collected, and yields primarily unilamellar vesicles with median diameter of 0.25 µm, and intravesicular/extravesicular volume ratio of 18 µl/ml. Control vesicles (control-liposomes) were prepared using an equal amount of albumin or crude protein from *E. coli* not expressing RLIP76. ATP-dependent transport of ¹⁴C-DOX and ³H-DNPSG in the rec-RLIP76 reconstituted proteoliposomes was performed by rapid filtration technique using the exact protocol described by us previously [12]. Efficiency of delivery for proteoliposomes has been established previously [12,18].

2.9. Preparations of crude membrane fractions for Western blot analyses

Crude membrane fractions were prepared from the normal and cancer cell lines using established procedures as described previously [19]. Levels of RLIP76 protein in normal and

cancer cells was measured by Western blot and ELISA assay using anti-RLIP76 IgG as previously described [18,19]. Purified rec-RLIP76 with purity assessed by amino acid composition analysis was used to generate calibration curves.

2.10. Transport studies in IOVs

Crude membrane vesicles (inside-out vesicles, IOV) were prepared from the normal (HAVSMC and HUVEC) and malignant (H82, H226, Caki-2, PC-3 and SW-480) cell lines using established procedures as described by us for the K562 cells [12,20]. Transport studies of DOX and DNP-SG in IOV were performed by the method as described previously [20]. ATP-dependent uptake of ^{14}C -DOX was determined by subtracting the radioactivity (cpm) of the control without ATP from that of the experimental containing ATP and the transport of DOX was calculated in terms of pmol/min/mg IOV protein. The transport of ^3H -DNP-SG was measured in a similar manner.

2.11. Animal model

Hsd: Athymic nude nu/nu mice (~12 weeks old) were obtained from Harlan, Indianapolis, IN. All animal experiments were carried out in accordance with a protocol approved by the Institutional Animal Care and Use Committee (IACUC). Twenty-four mice were divided into six groups of 4 animals (treatments with pre-immune serum, scrambled siRNA, scrambled anti-sense DNA, RLIP76 antibodies, RLIP76 siRNA and RLIP76 antisense). All 24 animals were injected with 2×10^6 human prostate cancer cells (PC-3) suspensions in 100 μl of PBS, subcutaneously into one flank of each mouse. Animals were examined daily for signs of tumor growth. Treatment were administered when the tumor surface area exceeded $\sim 42 \text{ mm}^2$ (~ day 27). Treatment consisted of 200 μg of RLIP76 antibodies, siRNA or antisense in 100 μl PBS. Control groups were treated with 200 μg /100 μl pre-immune serum, scrambled siRNA or scrambled anti-sense DNA. Tumors were measured in two dimensions by calipers using Study Director Software V1.6, from Studylog System, San Francisco, CA.

2.12. Colony forming assay

Cells (0.1×10^6 cells/500 μl) were irradiated at 100, 200, 500 and 1000 cGY using Varian Clinac 2100C Linear Accelerator with 6 MeV photon beam, for 1.25 min at the Texas Cancer Center, Arlington, TX, then aliquots 50 and 100 μl in 60 mm size petri dishes, separately, in a total volume of 4 ml by adding medium in each Petri dish. After 7 days, un-irradiated and irradiated cells were stained with methylene blue for 30 min. and colonies were counted using Innotech Alpha Imager HP [21].

2.13. Effect of RLIP76 antibody, siRNA and antisense on apoptosis by TUNEL assay

In these studies, we assessed whether cellular levels of RLIP76 could be depleted by RLIP76 antibody, siRNA or antisense mediated delivery to cultured prostate cancer cells, and assessed whether uptake is correlated with apoptosis by the TUNEL assay. The PC-3 prostate cancer cells (1×10^6 cells) were grown on the cover slips. The cells were treated with

RLIP76 antibody (40 $\mu\text{g}/\text{ml}$ final conc.) or transfected with either RLIP76 siRNA (20 $\mu\text{g}/\text{ml}$ final conc.) or RLIP76 antisense (10 $\mu\text{g}/\text{ml}$ final conc.). After 24 h incubation, the medium was removed, and cells were washed with PBS. TdT-mediated dUTP nick end labeling (TUNEL) assay was performed using Promega fluorescence detection kit according to the protocol provided by the manufacturer and described by us previously [21]. Briefly, cells were fixed by immersing slides in freshly prepared 4% paraformaldehyde solution for 30 min at 4°C followed by washing with PBS. The cells were permeabilized by immersing the slides in 0.2% Triton X-100 solution in PBS for 5 min followed by washing with PBS. Cells were equilibrated with equilibration buffer (provided by Promega Company) for 10 min. The equilibrated areas were blotted with tissue paper and TdT incubation buffer was added to the cells, and placed in humidified chamber. The chamber was covered with aluminum foil to protect from direct light. Slides were incubated at 37°C for 60 min and the reaction was terminated by immersing the slides in $2\times$ SSC buffer for 15 min followed by washing with PBS. The slides were stained in propidium iodide solution for 10 min in the dark and washed with distilled water several times. Slides were analyzed under a fluorescence microscope using a standard fluorescein filter set to view the green fluorescence at 520 nm, and red fluorescence of propidium iodide at $>620 \text{ nm}$. Fluorescence micrographs were taken using Zeiss LSM 510 META (Germany) laser scanning fluorescence microscope at $400\times$ magnification.

2.14. Statistical methods

All data were evaluated with a two-tailed unpaired student's *t* test or compared by one-way ANOVA and are expressed as the mean \pm SD. A value of $P < 0.05$ was considered statistically significant.

3. Results and discussion

3.1. Expression of RLIP76

Western-blot analyses of membrane protein extracts from various human normal and cancer cells were performed against anti-RLIP76 IgG indicated relatively larger amounts of RLIP76 in cancer versus normal cells (Fig. 1).

The results of RLIP76 protein and transport-activity are presented in Table 1 show that the amounts of total crude membrane proteins obtained from 100×10^6 cells in log-phase growth were comparable for normal and cancer cells. RLIP76 protein represented 0.21% and 0.66% of the total detergent soluble protein from the membranes of normal and cancer cells, respectively. These values of % of total membrane protein are in the range of those seen in various cell lines previously [15,19]. We have shown that proteoliposomes reconstituted with RLIP76, mediate ATP-dependent transport of DOX and other drugs [12,17,22]. In order to examine whether differential RLIP76 protein in normal and cancer cells was reflected in their transport activity, we compared the ATP-dependent uptake of DOX and DNP-SG in crude membrane inside-out vesicles (IOV) prepared separately from the mem-

Table 1 – RLIP76 protein and transport activity in human normal and cancer cells.

	Total crude protein (mg/10 ⁸ cells)	RLIP76 protein		Transport-activity (pmol/min/mg)	
		μg/10 ⁸ cells	% of total crude protein	¹⁴ C-DOX	³ H-DNP-SG
<i>Non-malignant</i>					
HAVSMC (aorta smooth muscle)	7.73 ± 0.61	17 ± 2	0.22	38 ± 5	114 ± 10
HUVEC (umbilical endothelial)	7.14 ± 0.48	15 ± 2	0.21	33 ± 5	104 ± 12
<i>Malignant</i>					
Caki-2 (kidney)	7.21 ± 0.72	44 ± 3	0.61	189 ± 12	684 ± 54
H-82 (lung, SCLC)	7.08 ± 0.47	34 ± 3	0.48	102 ± 8	316 ± 21
PC-3 (prostate)	7.88 ± 0.68	52 ± 3	0.66	257 ± 18	946 ± 42
H-226 (lung, NSCLC)	7.17 ± 0.82	38 ± 3	0.53	174 ± 14	594 ± 32
SW-480 (colon)	7.91 ± 0.86	49 ± 3	0.62	228 ± 21	744 ± 41

Cell lines were cultured in respective medium and homogenate was prepared from 100 × 10⁶ cells. RLIP76 was purified from total crude membrane fraction using DNPSG-affinity column chromatography, and quantified by ELISA. For transport studies, in-side-out vesicles (IOV) prepared from 20 × 10⁶ cells was enriched for IOVs by wheat-germ-agglutinin affinity chromatography [20]. Transport-activity was calculated from measurements of uptake of ¹⁴C-DOX (sp. activity, 8.5 × 10⁴ cpm/nmol) and ³H-DNP-SG (sp. activity, 3.6 × 10³ cpm/nmol) into the IOVs (20 μg/30 μl reaction mixture) in the absence or presence of 4 mM ATP. Each transport experiment was done in triplicates in three separate experiments (n = 9).

branes of control and cancer cells. The results presented in Table 1 clearly demonstrated that the ATP-dependent transport of DOX and DNP-SG was significantly higher in IOVs prepared from cancer cells than from normal cells. Results of

measurements of ATP-dependent transport of ¹⁴C-DOX and ³H-DNPSG revealed greater transport of both substrates in cancer cells containing greater amounts of RLIP76 protein, and a general correlation between RLIP76 protein level and transport-activity. Thus, greater RLIP76 expression corresponded to greater transport-activity.

3.2. Relative contribution of RLIP76 towards DOX-transport

DOX is a common allocrite transported by RLIP76 [12,18], MRP1 [23,24] and MDR1 [25]. We therefore, quantified the relative contribution of these transporters in the ATP-dependent transport of DOX in PC-3 cells using an immunological approach. We have previously shown that anti-RLIP76 IgG inhibit DOX-transport in IOVs [20,26]. Likewise, antibodies against MRP and Pgp also inhibit transport-activity in IOVs [26–28]. We therefore, designed experiments in which IOVs prepared from PC-3 cells and separately coated with anti-RLIP76 IgG, anti-MRP1 IgG, or anti-MDR1 IgG were used to measure the ATP-dependent uptake of ¹⁴C-DOX. Optimal concentration of antibody to be used for specific inhibition of DOX-transport was determined in titration studies where varying concentration of each antibody was used to coat the membrane-vesicles. Anti-RLIP76 IgG, which recognized only RLIP76 in crude extracts of PC-3 cells, inhibited 61 ± 8% of total DOX-transport in IOVs prepared from PC-3 cells. Anti-MRP IgG also inhibited DOX-transport in a saturable manner, but maximal inhibition was less (28 ± 5%) as compared to that observed with anti-RLIP76 IgG. Anti-Pgp IgG had a small but detectable inhibitory effect on DOX-transport (5 ± 2%). These results also established that <40 μg/ml of each of the antibody quantitatively inhibited transport-activity of their respective antigen present in the amount of vesicles used in these experiments. In the vesicle coated with the mixture of the three antibodies almost complete abrogation (92 ± 6%) of DOX-transport was observed. In control vesicles coated with pre-immune IgG, the transport-activity remained unaffected. These results demonstrated that RLIP76, MRP, and Pgp together

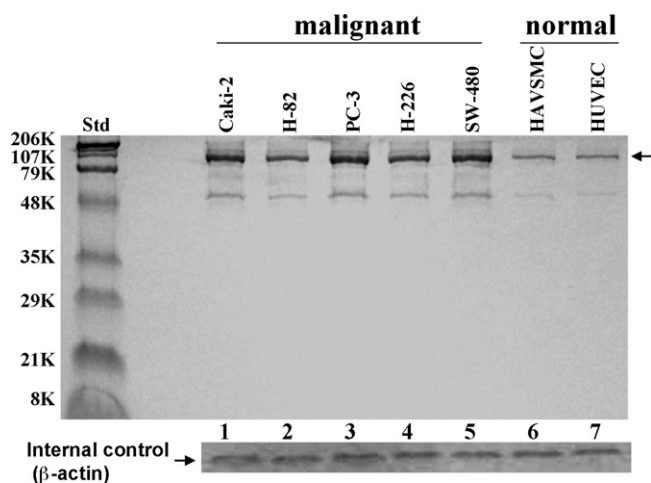


Fig. 1 – Comparison of RLIP76 levels in cultured malignant versus non-malignant cells. Aliquots of crude membrane fractions of malignant cells (human kidney, Caki-2; small cell lung, H-82; prostate, PC-3; non-small cell lung, H-226 and colon, SW-480) and non-malignant cells (human aortic vascular-smooth-muscle cells, HAVSMC and human umbilical vascular-endothelial cells, HUVEC) containing 200 μg protein were used for SDS-PAGE and Western-blotting against anti-RLIP76-IgG as primary-antibody and horseradish peroxidase-conjugated goat-anti-rabbit-IgG as secondary-antibody and developed with 4-chloro-1-naphthol as chromogenic substrate. Intensity of the full-length RLIP76 protein (~95 kDa, denoted by arrow) band was quantified by scanning densitometry as shown by integrated density values (IDV), for lanes 1–7 values are 32,259, 25,588, 35,597, 27,810, 33,377, 11,569, and 11,124, respectively, using Innotech Alpha Imager HP. β-actin was used as an internal control.

constitute nearly all ATP-dependent transport-activity in these membranes. Furthermore, these results established that RLIP76 accounted for a major portion (about two-third) of the ATP-dependent transport of DOX in prostate cancer cells.

3.3. RLIP76 inhibition or depletion caused cytotoxicity in malignant cells

The cytotoxic effects of RLIP76 inhibition by anti-RLIP76 IgG or the depletion of RLIP76 by either siRNA or antisense phosphorothioate were assessed by an established MTT-cytotoxicity method [13,18,19]. Cells were treated with pre-immune IgG, scrambled siRNA, scrambled antisense, anti-RLIP76 IgG, RLIP76 siRNA or RLIP76 antisense for 24 h. The preferential toxicity of all three targeting agents was preferentially directed to the malignant cells as compared with non-malignant cells, an observation we have seen with other malignant (lung, ovary, melanoma, breast) as compared with non-malignant cell lines [13,19]. In contrast with the results seen with lung or colon cancer previously (in which all three modalities gave similar results), antisense was significantly more effective in killing prostate cancer cells than the antibody (Fig. 2); this difference could be related to factors in prostate cancers that reduce the effectiveness of the antibody, or perhaps due a relatively greater role of some intracellular function of RLIP76 in prostate cancers.

3.4. Apoptosis caused by inhibition or depletion of RLIP76

The mechanism of cytotoxicity was assessed by determining apoptosis through an immuno-histochemical TUNEL assay.

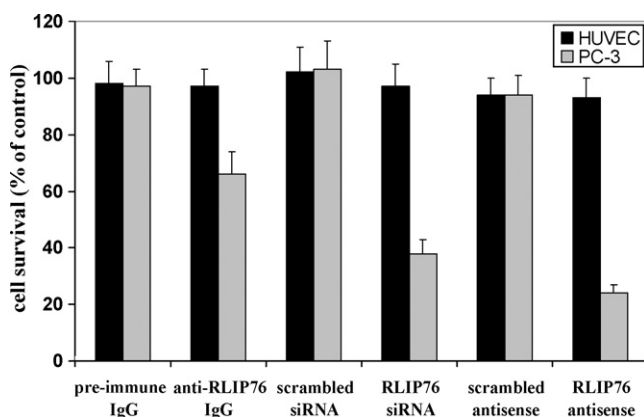


Fig. 2 – Selective toxicity of anti-RLIP76 IgG, RLIP76 siRNA and RLIP76 antisense toward PC-3 prostate cancer cells
Effect of anti-RLIP76 IgG (40 μ g/ml final concentration) on cell survival was determined by MTT assay. Depletion of RLIP76 expression by RLIP76 siRNA (20 μ g/ml final conc.) and RLIP76 antisense (10 μ g/ml final conc.) was done, using Transmessenger Transfection-Reagent-kit (Qiagen), and Maxfect Transfection-Reagent (Molecular, Inc.), according to the manufacturer's instructions, respectively. Cell survival was measured by MTT cytotoxicity-assay 48 h after treatment [18]. The values are presented as mean \pm SD from two separate determinations with eight-replicates each ($n = 16$). black bars, HUVEC (normal) cells; gray bars, PC-3 prostate cancer cells.

The results of the TUNEL assay showed no detectable apoptosis in the PC-3 cells treated with pre-immune IgG, scrambled siRNA or scrambled antisense. Apoptosis was however, seen in cells treated with anti-RLIP76 IgG, RLIP76 siRNA or RLIP76 antisense (Fig. 3A).

3.5. RLIP76 depletion caused regression of prostate cancer xenografts in nude mice

The ultimate pre-clinical test for the potential utility of an anti-neoplastic agent is effectiveness in an animal model. The above observations of the anti-neoplastic effects of RLIP76 depletion were examined in a xenografts model of prostate cancer. Tumor-bearing animals with established s.c. implanted tumors ($\sim 42 \text{ mm}^2$) were treated with 200 μ g of either RLIP76 antibody, RLIP76 siRNA or RLIP76 antisense therapy by i.p. injection. Treated animals had rapid and dramatic reductions in tumors, whereas uncontrolled growth was observed in the control groups. The remarkable contrast in the outcome of tumors in animals treated with RLIP76 antibody, RLIP76 siRNA or RLIP76 antisense versus pre-immune serum, scrambled siRNA or antisense was clearly evident for prostate cancer cell lines (Fig. 3B) (for animal pictures, see supplementary data). The RLIP76 antibody, RLIP76 siRNA or RLIP76 antisense treated animals with prostate cancer are still alive at 261 days without evidence of recurrence. In comparison, all control animals were censored by day 41. Weight gain was comparable to non-tumor-bearing controls, and no overt-toxicity was evident. Present studies demonstrate nearly complete and sustained regression of xenografts of PC-3 prostate cancer by targeted depletion of the mercapturic acid pathway transporter protein, RLIP76.

The marked effectiveness of this targeted therapy compares quite favorably with other promising targeted agents in prostate cancer. ZD6126, a vascular targeting agent, caused reduction in the growth of xenografts in nude mice when administered by i.v. (100 mg/kg) daily for 5 days, resulted in $\sim 18\%$ body weight loss; the combination of cisplatin and ZD6126 resulted in greater than additive in growth delay, but regression was not observed [29]. Vitamin D3 analog (1,25-dihydroxyvitamin D3), anti-PSMA (prostate specific membrane antigen) and anti-interleukin-6 (IL-6) monoclonal antibodies were found effective in xenografts of LNCaP prostate cancer carcinoma, but growth inhibition occurred rather than regression [30–32]. PTEN (phosphatase and tensin homolog), a protein known to inhibit Bcl-2 expression, caused reduction in the rate of growth of PC-3 xenografts; the combination of PTEN with radiation therapy (5 Gy) was more effective in slowing growth, but regression was not observed [33]. CKBM is a combination of herbs and yeasts, a drug product targeting prostate cancer, did cause delayed and incomplete regression by 28 days in xenografts of PC-3 prostate cell carcinoma, when treatment was started before established visible tumor was present [34]. Polyamine analogues containing cyclopropane rings caused reduction in the rate of growth of DU-145 prostate cancer xenografts, but regression was not observed [35]. Combination of doxorubicin (4 mg/kg, i.p.) and Apo2L/TRAIL (0.5 mg/kg, i.p.) did cause regression of very small tumors, but if treatment was started at the time of established PC-3 prostate tumors at least 6 mm in each dimension (as in our case), only relatively little growth inhibition was seen [36]. The

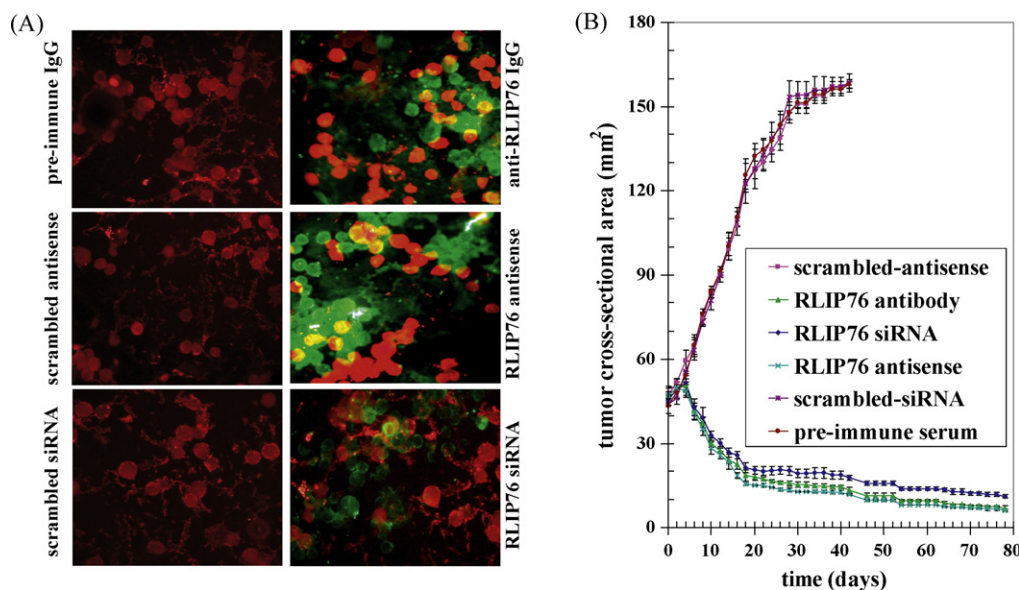


Fig. 3 – Effect of RLIP76 antibody, siRNA or antisense on apoptosis and on the regression of established PC-3 prostate cancer xenografts Effect of anti-RLIP76 IgG, RLIP76 siRNA and RLIP76 antisense on apoptosis was performed by TUNEL assay. Human prostate cancer cells were grown on cover-slips. For anti-RLIP76 IgG treatment, cells were incubated with RLIP76 antibody for 24 h; for siRNA treatment, cells were transfected with Transmessenger Transfection Reagent (Qiagen); for antisense treatment, cells were transfected with Maxfect Transfection Reagent (Molecular, Inc.), prior to TUNEL assay, using Promega fluorescence detection kit and examined using Zeiss LSM 510 META (Germany) laser scanning fluorescence microscope with filters 520 nm and >620 nm. Photographs taken at identical exposure at 400× magnification are presented. Apoptotic cells showed green fluorescence (panel A). For xenografts studies, we used twenty-four 12-week-old Hsd: Athymic nude nu/nu mice (Harlan, Indianapolis, IN) randomized 4 animals each into six groups as follow: (1) pre-immune serum, (2) scrambled siRNA, (3) scrambled anti-sense DNA, (4) RLIP76 antibodies, (5) RLIP76 siRNA and (6) RLIP76 antisense. All 24 animals were injected with 2×10^6 human prostate cancer cells (PC-3) suspensions in 100 μ l of PBS, subcutaneously into one flank of each nu/nu nude mouse. Animals were examined daily for signs of tumor growth. When tumors reached a cross-sectional area of ~ 42 mm² (27 days later), animals were randomized treatment groups as indicated in the figure (for animal pictures, see [supplementary data](#)). Treatment consisted of 200 μ g of RLIP76 antibodies, siRNA or antisense in 100 μ l PBS. Control groups were treated with 200 μ g/100 μ l pre-immune serum, scrambled siRNA or scrambled anti-sense DNA. Tumors were measured in two dimensions using calipers. Tumor measurements are presented with all control groups (pre-immune IgG, scrambled siRNA or antisense) versus all treated groups (anti-RLIP76 IgG, RLIP76 siRNA, or anti-sense) (panel B).

therapeutic and toxicological effect of cesium chloride (~ 1000 mg/kg by oral gavage for 30 consecutive days) administration has recently been shown to nearly completely inhibit the growth of established PC-3 cell lines in xenografts, but also did not cause regression. Cesium chloride had no effect on LNCaP tumors [37]. Incomplete regression was seen by day 32 in xenografts of PC-3 cell carcinoma treated with 2-methoxyestradiol (2ME2, 75 mg/kg, p.o.) and 2 Gy radiation delivered each day for 5 days inhibits microtubule polymerization and angiogenesis, and celecoxib, COX-2 inhibitor [38,39]. Thus, targeted therapeutics for prostate cancer aimed at Bcl-2, 2ME2, COX-2, CKBM, IL-6, Apo2L/TRAIL, or PTEN do not appear as effective as RLIP76 inhibition or depletion in comparable animal xenografts models.

3.6. Radiation-sensitivity

We have shown that RLIP76 knockout mice are extremely sensitive to irradiation [10,40], and in recent studies, we have also demonstrated that the overall effect of RLIP76-depletion is

almost an order of magnitude greater than the effects exerted by important signaling proteins including Akt, JNK and MEK [10]. Based on these previous studies in knockout-animals and other histologies of cancer cells, we reasoned that RLIP76 modulation would directly affect radiation-sensitivity and resistance of prostate cancer cells. To test this postulate, we determined X-irradiation sensitivity of the human prostate cancer cells in dose-response studies utilizing 100–1000 cGY single dose X-irradiation, followed by colony-forming assays. Cells pretreated with RLIP76-liposomes were least sensitive to radiation. Delivery of RLIP76 to cells via a liposomal-delivery system completely reversed radiation-sensitivity. At each radiation-dose, survival was significantly more when the cells were pretreated with RLIP76-liposomes before radiation exposure (Fig. 4). The physiological significance of RLIP76-mediated transport of endogenously generated GS-E (e.g., conjugate of 4HNE) is further indicated by results of our studies showing that RLIP76-enriched cells are resistant to radiation-toxicity. In these studies, prostate cancer cells were loaded with RLIP76 by incubating with RLIP76-liposomes. As

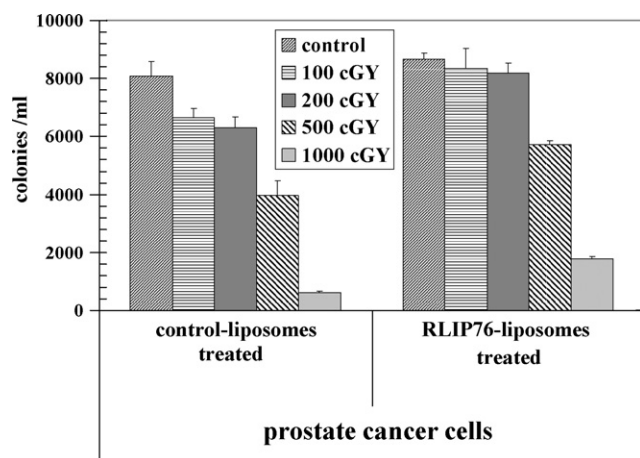


Fig. 4 – Radiation-protection by RLIP76 liposomal delivery 2.5×10^3 human prostate cancer cells grown in Ham's F12 medium, were treated with control and RLIP76-liposomes (50 μ g/ml final conc.) for 24 h prior to radiation at 100, 200, 500 and 1000 cGY (6 MeV photons, 1.25 min) at the Texas Cancer Center, Arlington, TX. After 7 days, cells were stained with methylene-blue and the colonies were counted using Alpha Imager HP [21]. The results presented are the mean and s.d. from three separate experiments.

shown in Fig. 4, cells enriched with RLIP76 were resistant to radiation as compared to controls. These results suggest that the electrophilic-products of lipid-peroxide caused by reactive-oxygen species (ROS) generated during radiation may account for the cell killing by radiation and that RLIP76-mediated transport of GSH-conjugates of these electrophiles provides protection from radiation. These findings confirmed prior findings that RLIP76-liposomes are excellent radio-protective agents [10,40].

Cancer therapy target proteins must be expressed differentially in cancer as compared with normal cells, and the necessity for the presence of the target protein must differ between cancers vs. normal cells. Ideally, the target should be understood in context of existing biochemical and physiological frameworks and pathways known to play a direct role in carcinogenesis or in thwarting cancer therapy. In the present studies, we demonstrate that RLIP76 is a very promising target for therapy of prostate and other cancers, but important additional mechanistic and pre-clinical data is necessary to understand the role of RLIP76 in regulating key signaling pathways known to be important in carcinogenesis, drug-resistance, and the mechanisms of intrinsic drug-resistance in cancer. Other investigators have shown that binding of cdc2 to RLIP76 is essential to shut off endocytosis during mitosis, and yet others that over-expression of POB1 (partner of RLIP76) triggers apoptosis in prostate cancer cells [41,42]. Results of our present studies are in strong support of our hypothesis that prostate cancer cell depend on the function of RLIP76 for survival. The RLIP76 antibody, siRNA or antisense, is a novel and promising therapeutic agent for the treatment of human prostate cancers. Further studies are required to elucidate its mechanism of action.

4. Conclusions

The results of the present study clearly demonstrate that RLIP76 protein and activity is greater in cancer cells as compared with normal cells and that apoptosis triggered by RLIP76 depletion will be manifested preferentially in cancer as compared with normal cells. Studies demonstrating the marked enhancement of vinorelbine efficacy in lung cancer xenografts by concomitant depletion of RLIP76 have confirmed the *in vivo* relevance of these observations [13]. Present studies have shown that human cancers (lung, colon, kidney and prostate) express higher levels of RLIP76 than non-cancerous cell, and that depletion or inhibition of RLIP76 in these cancer cell types caused marked apoptosis, whereas non-cancerous cells were spared. Because human prostate cancers have a relatively high expression of RLIP76, we reasoned that it may be functioning as a defense mechanism in prostate cancer cells as well. RLIP76 plays a central role in radiation and chemotherapy-resistance through its activity as a multi-specific ATP-dependent transporter. In conclusion, present studies demonstrate that depletion of RLIP76 exerts anti-neoplastic effects in prostate cancer. This study should help lay the foundation for clinical studies. These outstanding findings will have obvious translational implications for the treatment of prostate cancer and potentially other malignancies.

Acknowledgements

This work was supported in part by National Institutes of Health Grants CA 77495 and CA 104661, Cancer Research Foundation of North Texas, Institute for Cancer Research and the Joe & Jessie Crump Fund for Medical Education.

Appendix A. Supplementary data

Supplementary data associated with this article can be found, in the online version, at [doi:10.1016/j.bcp.2008.11.013](https://doi.org/10.1016/j.bcp.2008.11.013).

REFERENCES

- [1] Sirotnak FM, Wendel HG, Bornmann WG, Tong WP, Miller VA, Scher HI, et al. Co-administration of probenecid, an inhibitor of a cMOAT/MRP-like plasma membrane ATPase, greatly enhanced the efficacy of a new 10-deazaaminopterin against human solid tumors *in vivo*. *Clin Cancer Res* 2000;6:3705–12.
- [2] Zhang Y, Bressler JP, Neal J, Lal B, Bhang HE, Laterra J, et al. ABCG2/BCRP expression modulates D-Luciferin based bioluminescence imaging. *Cancer Res* 2007;67:9389–97.
- [3] Grant S. Cotargeting survival signaling pathways in cancer. *J Clin Invest* 2007;118:3003–6.
- [4] Shen MM, Abate-Shen C. Pten inactivation and the emergence of androgen-independent prostate cancer. *Cancer Res* 2007;67:6535–8.
- [5] Kinkade CW, Castillo-Martin M, Puzio-Kuter A, Yan J, Foster TH, Gao H, et al. Targeting AKT/mTOR and ERK MAPK signaling inhibits hormone-refractory prostate cancer in a preclinical mouse model. *J Clin Invest* 2008;118:3051–64.

- [6] Pusztai L, Wagner P, Ibrahim N, Rivera E, Theriault R. Phase II study of tariquidar, a selective P-glycoprotein inhibitor, in patients with chemotherapy-resistant, advanced breast carcinoma. *Cancer* 2005;104:682–91.
- [7] Modok S, Mellor HR, Callaghan R. Modulation of multidrug resistance efflux pump activity to overcome chemoresistance in cancer. *Curr Opin Pharmacol* 2006;6:350–4.
- [8] Robey RW, Shukla S, Finley EM, Oldham RK, Barnett D, Ambudkar SV, et al. Inhibition of P-glycoprotein (ABCB1)- and multidrug resistance-associated protein 1 (ABCC1)-mediated transport by the orally administered inhibitor, CBT-1((R)). *Biochem Pharmacol* 2008;75:1302–12.
- [9] Shukla S, Wu CP, Ambudkar SV. Development of inhibitors of ATP-binding cassette drug transporters: present status and challenges. *Expert Opin Drug Metab Toxicol* 2008;4: 205–23.
- [10] Singhal J, Singhal SS, Yadav S, Warnke M, Yacoub A, Dent P, et al. RLIP76 in defense of radiation poisoning. *Int J Rad Oncol Biol Phys* 2008;72:553–61.
- [11] Jullien-Flores V, Dorseuil O, Romero F, Letourneur F, Saragosti S, Berger R, et al. Bridging Ral-GTPase to Rho-pathways. RLIP76, a Ral-effector with CDC42/RacGTPase activating protein activity. *J Biol Chem* 1995;270:22473–7.
- [12] Awasthi S, Cheng J, Singhal SS, Saini MK, Pandya U, Pikula S, et al. Novel function of human RLIP76: ATP-dependent transport of glutathione-conjugates and doxorubicin. *Biochemistry* 2000;39:9327–34.
- [13] Singhal SS, Singhal J, Yadav S, Dwivedi S, Boor P, Awasthi YC, et al. Regression of lung and colon cancer xenografts by depleting or inhibiting RLIP76. *Cancer Res* 2007;67: 4382–9.
- [14] Awasthi YC, Garg HS, Dao DD, Partridge CA, Srivastava SK. Enzymatic conjugation of erythrocyte glutathione with 1-chloro-2,4-dinitrobenzene: the fate of glutathione conjugate in erythrocytes and the effect of glutathione depletion on hemoglobin. *Blood* 1981;58:733–8.
- [15] Singhal SS, Singhal J, Sharma R, Singh SV, Zimniak P, Awasthi YC, et al. Role of RLIP76 in lung cancer doxorubicin-resistance. I. The ATPase activity of RLIP76 correlates with doxorubicin and 4HNE-resistance in lung cancer cells. *Int J Oncol* 2003;22:365–75.
- [16] Awasthi S, Singhal SS, Sharma R, Zimniak P, Awasthi YC. Transport of glutathione-conjugates and chemotherapeutic drugs by RLIP76: a novel link between G-protein and tyrosine-kinase signaling and drug-resistance. *Int J Cancer* 2003;106:635–46.
- [17] Stuckler D, Singhal J, Singhal SS, Yadav S, Awasthi YC, Awasthi S. RLIP76 transports vinorelbine and mediates drug-resistance in non-small cell lung cancer. *Cancer Res* 2005;65:991–8.
- [18] Singhal SS, Yadav S, Singhal J, Zajac E, Awasthi YC, Awasthi S. Depletion of RLIP76 sensitizes lung cancer cells to doxorubicin. *Biochem Pharmacol* 2005;70:481–8.
- [19] Singhal SS, Awasthi YC, Awasthi S. Regression of melanoma in a murine model by RLIP76-depletion. *Cancer Res* 2006;66:2354–60.
- [20] Awasthi S, Singhal SS, Srivastava SK, Zimniak P, Bajpai KK, Saxena M, et al. Adenosine-triphosphate-dependent transport of doxorubicin, daunomyicin, and vinblastine in human tissues by a mechanism distinct from the P-glycoprotein. *J Clin Invest* 1994;93:958–65.
- [21] Singhal SS, Yadav S, Drake K, Singhal J, Awasthi S. Hsf-1 and POB1 induce drug-sensitivity and apoptosis by inhibiting Ralbp1. *J Biol Chem* 2008;283:19714–29.
- [22] Sharma R, Singhal SS, Wickramarachchi D, Awasthi YC, Awasthi S. RLIP76-mediated transport of leukotriene C₄ in cancer cells: implications in drug-resistance. *Int J Cancer* 2004;112:934–42.
- [23] Cole SPC, Bhardwaj G, Gerlach JH, Mackie JE, Grant CE, Almquist KC, et al. Over-expression of a transporter gene in a multidrug-resistant human lung cancer cell line. *Science* 1992;258:1650–4.
- [24] Lautier D, Canitrot Y, Deeley RG, Cole SPC. Multidrug-resistance mediated by the multidrug-resistance protein (MRP) gene. *Biochem Pharmacol* 1996;52: 967–77.
- [25] Gottesman MM, Pastan I. Biochemistry of multidrug-resistance mediated by the multidrug-transporter. *Annu Rev Biochem* 1993;62:385–427.
- [26] Awasthi S, Singhal SS, Singhal J, Cheng J, Zimniak P, Awasthi YC. Role of RLIP76 in lung cancer doxorubicin-resistance. II. Doxorubicin-transport in lung cancer by RLIP76. *Int J Oncol* 2003;22:713–20.
- [27] Hipfner DR, Mao Q, Qiu W, Leslie EM, Gao M, Deeley RG, et al. Monoclonal-antibodies that inhibit the transport function of the 190-kDa multidrug-resistance protein, MRP. Localization of their epitopes to the nucleotide-binding-domains of the protein. *J Biol Chem* 1999;274: 15420–6.
- [28] Kokubu N, Cohen D, Watanabe T. Functional modulation of ATPase of P-glycoprotein by C219, a monoclonal-antibody against P-glycoprotein. *Biochem Biophys Res Commun* 1997;230:398–401.
- [29] Blakey DC, Westwood FR, Walker M, Hughes GD, Davis PD, Ashton SE, et al. Antitumor activity of the novel vascular targeting agent ZD6126 in a panel of tumor models. *Clin Cancer Res* 2002;8:1974–83.
- [30] Vegesna V, O'Kelly J, Said J, Uskokovic M, Binderup L, Koeffle HP. Ability of potent vitamin D3 analogs to inhibit growth of prostate cancer cells in vivo. *Anticancer Res* 2003;23:283–9.
- [31] Vallabhajosula S, Smith-Jones PM, Navarro V, Goldsmith SJ, Bander NH. Radio-immunotherapy of prostate cancer in human xenografts using monoclonal antibodies specific to prostate specific membrane antigen (PSMA): studies in nude mice. *Prostate* 2004;58:145–55.
- [32] Smith PC, Keller ET. Anti-interleukin-6 monoclonal antibody induces regression of human prostate cancer xenografts in nude mice. *Prostate* 2001;48:47–53.
- [33] Anai S, Goodison S, Shiverick K, Iczkowski K, Tanaka M, Rosser CJ. Combination of PTEN gene therapy and radiation inhibits the growth of human prostate cancer xenografts. *Hum Gene Ther* 2006;17:975–84.
- [34] Liu ES, Luk SC, Leung ET, Lee WH, Yuen WF, Kwok KM, et al. Effect of CKBM on prostate cancer cell growth in vitro and in vivo. *J Chemother* 2008;20:246–52.
- [35] Frydman B, Blokhin AV, Brummel S, Wilding G, Maxuitenko Y, Sarkar A, et al. Cyclopropane-containing polyamine analogues are efficient growth inhibitors of a human prostate tumor xenograft in nude mice. *J Med Chem* 2003;46:4586–600.
- [36] El-Zawahry A, McKillop J, Voelkel-Johnson C. Doxorubicin increases the effectiveness of Apo2L/TRAIL for tumor growth inhibition of prostate cancer xenografts. *BMC Cancer* 2005;5:2.
- [37] Low JC, Wasan KM, Fazli L, Eberding A, Adomat H, Guns ES. Assessing the therapeutic and toxicological effects of cesium chloride following administration to nude mice bearing PC-3 or LNCaP prostate cancer xenografts. *Cancer Chemother Pharmacol* 2007;60:821–9.
- [38] Casarez EV, Dunlap-Brown ME, Conaway MR, Amorino GP. Radio-sensitization and modulation of p44/42 mitogen-activated protein kinase by 2-Methoxyestradiol in prostate cancer models. *Cancer Res* 2007;67: 8316–24.
- [39] Patel MI, Subbaramaiah K, Du B, Chang M, Yang P, Newman RA, et al. Celecoxib inhibits prostate cancer growth:

- evidence of a cyclooxygenase-2-independent mechanism. *Clin Cancer Res* 2005;11:1999–2007.
- [40] Awasthi S, Singhal SS, Yadav S, Singhal J, Drake K, Nadkar A, et al. RLIP76 is a major determinant of radiation-sensitivity. *Cancer Res* 2005;65:6022–8.
- [41] Oosterhoff JK, Penninkhof F, Brinkmann AO, Grootegoed JA, Blok LG. POB1 is down-regulated during human prostate cancer progression and inhibits growth factor signaling in prostate cancer cells. *Oncogene* 2003;22:2920–5.
- [42] Rosse C, L'Hoste S, Offner N, Picard A, Camonis JH. RLIP, an effector of the Ral-GTPases, is a platform for Cdk1 to phosphorylate epsin during the switch off of endocytosis in mitosis. *J Biol Chem* 2003;278:30597–604.